THE JOURNAL OF PHYSICAL CHEMISTRY B

Article

pubs.acs.org/JPCB

Temperature and Pressure Based NMR Studies of Detergent Micelle Phase Equilibria

Rohan Alvares,[†] Shaan Gupta,[†,∥] Peter M. Macdonald,[†] and R. Scott Prosser*[,†,§]

[†]Department of Chemistry, University of Toronto, UTM Campus, 3359 Mississauga Road North, Mississauga, Ontario, Canada L5L 1C6

[§]Department of Biochemistry, University of Toronto, Toronto, Ontario, Canada M5S 1A8

Supporting Information

ABSTRACT: Bulk thermodynamic and volumetric parameters (ΔG°_{mic}, ΔH°_{mic}, ΔS°_{mic}, $\Delta C^{\circ}_{p,mic}$, ΔV°_{mic}, and $\Delta\kappa^{\circ}_{mic}$) associated with the monomer−micelle equilibrium, were directly determined for a variety of common detergents [sodium *n*-dodecyl sulfate (SDS), *n*-dodecyl phosphocholine (DPC), *n*-dodecyl-*β*-D-maltoside (DDM), and 7-cyclohexyl-1-heptyl phosphocholine (CyF)] via ^{1}H NMR spectroscopy. For each temperature and pressure point, the critical micelle concentration (cmc) was obtained from a single ^{1}H NMR spectrum at a single intermediate concentration by referencing the observed chemical shift to those of pure monomer and pure micellar phases. This permitted rapid measurements of the cmc over a range of temperatures and pressures. In all cases, micelle formation was strongly entropically favored, while enthalpy changes were all positive, with the exception of SDS, which exhibited a modestly negative enthalpy of micellization. Heat capacity changes were also characteristically negative, while partial molar volume changes were uniformly positive, as expected for an aggregation process dictated by hydrophobic effects. Isothermal compressibility changes were found to be consistent with previous measurements using other techniques. Thermodynamic measurements were also related to spectroscopic studies of topology and micelle structure. For example, paramagnetic effects resulting from the addition of dioxygen provided microscopic topological details concerning the hydrophobicity gradient along the detergent chains within their respective micelles as detected by ^{1}H NMR. In a second example, combined ^{13}C and ^{1}H NMR chemical shift changes arising from application of high pressure, or upon micellization, of CyF provided site-specific details regarding micelle topology. In this fashion, bulk thermodynamics could be related to microscopic topological details within the detergent micelle.

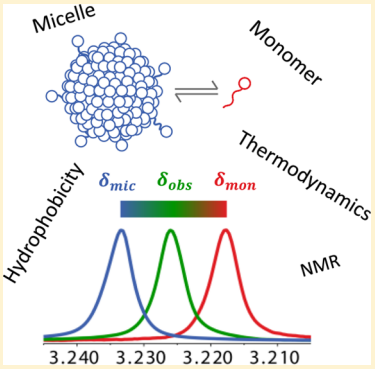

INTRODUCTION

In biological systems, many macromolecules, including proteins, DNA, fatty acids, and lipids, spontaneously adopt highly ordered aggregate structures. For amphiphilic molecules, such organization is driven largely by the hydrophobic effect. In this study, we measure the thermodynamic driving forces associated with the formation of micellar aggregates for a variety of detergents and relate these to their structural and topological properties.

A host of physical techniques are available to study micelle phase equilibria in water, including differential scanning[1] and isothermal titration calorimetry,[2] pressure perturbation calorimetry,[3] dielectric spectroscopy,[4] ultrasonic measurements,[5,6] and NMR spectroscopy.[7−12] In most cases, an equilibrium constant is obtained by measuring the dependence of some physical parameter of the system on detergent concentration under specific conditions of temperature, pressure, and ionic strength.

NMR is a particularly useful means to study detergent micelle phase equilibria since the detergents are invariably in very fast exchange (on NMR time scales) between the micelle and the monomer phases.[13] Hence, little exchange broadening is observed, and the NMR spectra may be interpreted in terms of a simple weighted average of the spectral signatures associated with the monomer and the micellar detergent fractions. This permits, in principle, direct evaluation of the critical micelle concentration (cmc) from a single detergent concentration. If repeated over a range of temperatures and pressures, then standard thermodynamic and volumetric parameters associated with the monomer−micelle equilibria such as changes in free energy (ΔG°_{mic}), enthalpy (ΔH°_{mic}), entropy (ΔS°_{mic}), heat capacity ($\Delta C^{\circ}_{p,mic}$), partial molar volume (ΔV°_{mic}), and isothermal compressibility ($\Delta\kappa^{\circ}_{mic}$) can be extracted.[6,14−21] The current limits of detection in NMR are such that it is possible to acquire reliable spectra from nanomolar quantities of detergent and thus, in principle, to measure cmc's up to this limit, so long as the fast exchange condition is met. Ultrasound and calorimetric methods, which rely upon a bulk property to distinguish monomer from micelle, become problematic for such very low cmcs.

NMR also provides a window into molecular and topological features associated with both single molecules and aggregates.[22]

Received: January 6, 2014
Revised: May 5, 2014
Published: May 6, 2014

dx.doi.org/10.1021/jp500139p | J. Phys. Chem. B 2014, 118, 5698−5706

For example, chemical shifts, and in particular, chemical shift changes upon micellization, can provide some sense of the tertiary environment, packing forces, and relative mobility of micelle constituents. Similarly, three-bond scalar coupling dihedral angles reveal average conformations[23] associated with detergents in their respective environments. In homonuclear ^{1}H nuclear Overhauser enhancement spectroscopy (NOESY) experiments, cross-peaks can provide insight into detergent−detergent and detergent−water contacts. Similarly, the paramagnetic enhancement of ^{1}H spin−lattice relaxation rates and/or paramagnetic shifts caused by paramagnetic additives, such as TEMPOL[24] or dioxygen,[25,26] gives an indication of the packing environment, local hydrophobicity, and solvent exposure of the nucleus of interest. Detergent dynamics in the micelle, ranging from rapid chain and headgroup isomerizations to molecular rotational diffusion and slower collective motions, may be examined using heteronuclear nuclear Overhauser effects (NOEs) and T_1 and T_2 relaxation measurements of both (natural abundance) ^{13}C and ^{1}H species.[22] Finally, pulsed field gradient (PFG) NMR diffusion techniques can provide a reliable measure of micelle aggregate sizes and hydrodynamic radii.[27−29] In principle, such information can be related to the thermodynamic properties of the system, thereby establishing a connection between the detergent structure and the properties of their micellar assemblies via a statistical mechanical formalism.

Herein, we demonstrate the potential of NMR to rapidly characterize thermodynamic and volumetric changes upon micellization and, in addition, to address molecular and topological properties of the micelle. First, we employ simple ^{1}H chemical shift changes associated with micelle formation to characterize cmc changes with temperature and pressure across a series of detergents having identical chain lengths and/or head groups, specifically sodium *n*-dodecyl sulfate (SDS), *n*-dodecyl phosphocholine (DPC), *n*-dodecyl-*β*-D-maltoside (DDM), and 7-cyclohexyl-1-heptyl phosphocholine (CyF). The structures of these various detergents are shown in Figure 1.

These temperature and pressure dependencies provide bulk thermodynamic and volumetric parameters associated with micellization. We next examine the hydrophobicity gradient within the micelle by measuring the relative partitioning of dioxygen into the micelle interior via its site-specific ^{1}H paramagnetic rate enhancements.[25,30,31] For the case of CyF, even greater site-specific details on packing density and micelle topology were obtained from combined ^{1}H and ^{13}C chemical shift changes upon micellization and pressure perturbations. Using such information, the thermodynamic and volumetric changes for different detergents can be related to topological features at a molecular level.

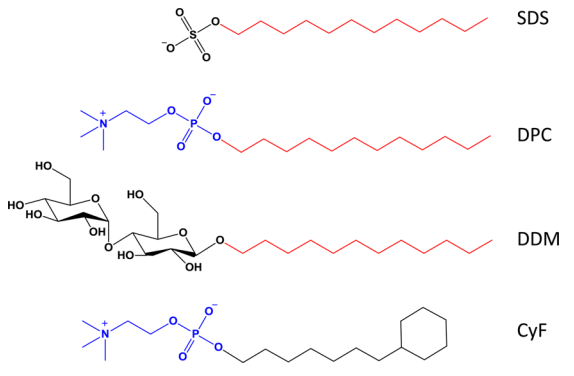

Figure 1. Structures of sodium *n*-dodecyl sulfate (SDS), *n*-dodecyl phosphocholine (DPC), *n*-dodecyl-*β*-D-maltoside (DDM), and 7-cyclohexyl-1-heptyl phosphocholine (CyF). SDS, DPC, and DDM possess identical hydrophobic tails (red), while DPC and CyF possess identical head groups (blue).

THEORY

In considering the equilibrium between detergent monomer and micelle, we begin by adopting the phase equilibrium model which assumes that the system is defined by either a monomeric or a micellar phase. At concentrations below the cmc, the entire system exists in the monomer phase, whereas above the cmc monomer and micelle phases coexist. The monomer mole fraction, X_{mon}, is obtained from the ratio between the cmc and the total detergent concentration.[32]

$$X_{mon} = \frac{cmc}{[detergent]} \quad (1)$$

Traditionally, the cmc is determined in NMR spectroscopy by monitoring a spectroscopic feature such as the chemical shift or line width as a function of concentration of detergent.[7,33] The resulting profile across the entire titration range is interpreted in terms of the mass action or phase equilibrium model to obtain an estimate of the cmc. However, for most detergents there is fast exchange on the NMR time scale between the micelle phase and the monomer phase. This means that an NMR observable such as the chemical shift is a population-weighted average over the chemical shift difference, $\Delta\nu$, between monomer and micelle resonances. For fast exchange, the condition $k_{ex} \gg 2\pi\Delta\nu$ must apply.[13] For a typical chemical shift difference of $\Delta\nu \leq 50$ Hz, this implies $k_{ex} > 500$ Hz. Assuming the fast exchange condition,[34] it is possible to estimate the cmc based on a single spectrum and two "end point" spectra corresponding to the pure monomer and pure micelle phases, respectively. In this instance, the observed chemical shift, δ_{obs}, for any detergent resonance is related to the mole fraction of monomer, X_{mon}, as per

$$\delta_{obs} = X_{mon}\delta_{mon} + (1 - X_{mon})\delta_{mic} \quad (2)$$

where δ_{mic} is the chemical shift associated with a pure micelle phase, and δ_{mon} is that associated with a pure monomer phase. Hence, the monomer mole fraction may be expressed entirely in terms of NMR observables.

$$X_{mon} = \frac{\delta_{obs} - \delta_{mic}}{\delta_{mon} - \delta_{mic}} \quad (3)$$

The chemical shifts associated with the pure phases, δ_{mon} and δ_{mic}, may be obtained by recording NMR spectra at concentrations 5−10 times below the cmc and, typically, 20 times above the cmc, respectively. The very low concentrations are chosen in order to avoid the presence of any intermediate phase, or premicelle state,[35] which might confound the preceding two-state analysis. Hence, the value of δ_{obs} provides a direct measure of the cmc, as illustrated in Figure 2 for the case of the choline methyl ^{1}H NMR resonance of DPC. Moreover, where several resonances in a given spectrum are sensitive to the monomer−micelle equilibrium, an average, $\langle X_{mon} \rangle$, may be obtained to improve the precision of an equilibrium measurement.

dx.doi.org/10.1021/jp500139p | J. Phys. Chem. B 2014, 118, 5698−5706

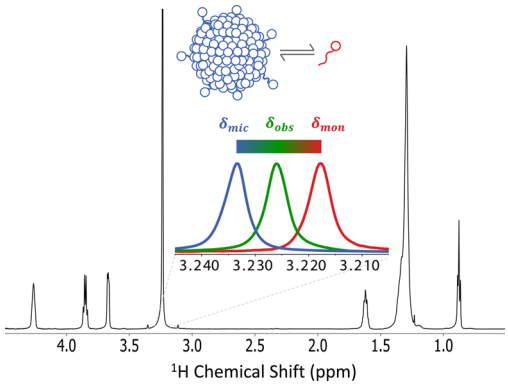

Figure 2. ^{1}H NMR spectrum of DPC (black). The inset shows three superimposed spectra of the DPC choline region. Due to fast exchange the observed spectrum (green; 3.226 ppm) represents a weighted average of spectra associated with the two distinct environments or phases: that of the pure micelle phase (blue; 3.233 ppm), obtained at a concentration well above the cmc, and that of the pure monomer phase (red; 3.218 ppm), obtained at a concentration well below the cmc. From the relative mole fractions of detergent in the micellar and monomeric phases, the cmc, and hence the monomer−micelle equilibrium constant, is determined. For the choline peaks, the change in chemical shift between the monomeric and micellar samples is, in this case, 9 Hz, whereas the full width at half-maximum (fwhm) is 3 Hz. However, larger (20−40 Hz) chemical shift changes are observed for all detergents (Supporting Information Table S1), and chemical shift changes from many peaks, of a given detergent, can be combined to further improve resolution and reduce error (see Data Analysis).

The free energy change associated with formation of the micelle phase from the monomer phase is then given by[15,18]

$$\Delta G^\circ_{\mathrm{mic}} = (1+f)RT\ln(X_{\mathrm{mon}}) \tag{4}$$

where R is the gas constant, T is temperature, and f represents the fraction of counterion associated with the micelle (*i.e.*, $f = 0$ for uncharged species and 1 when there is 100% counterion association). Equation 4 assumes that changes in micelle size with temperature may be ignored.[36]

The preceding equilibrium measurement can be extended readily in the temperature and pressure dimensions, thereby providing a wealth of thermodynamic and volumetric information associated with the monomer to micelle phase transition. The temperature dependence of the standard free energy change provides a measure of the changes in enthalpy, $\Delta H^\circ_{\mathrm{mic}}$, entropy, $\Delta S^\circ_{\mathrm{mic}}$, and heat capacity, $\Delta C^\circ_{p,\mathrm{mic}}$,[2,32]

$$\Delta G_{\mathrm{mic}} = \Delta H^\circ_{\mathrm{mic}} - T\Delta S^\circ_{\mathrm{mic}} + \Delta C^\circ_{p,\mathrm{mic}}[T - T^\circ - T\ln(T/T^\circ)] \tag{5}$$

where T° is the reference temperature. Similarly, the pressure dependence of the free energy change is related to changes in partial molar volume, $\Delta V^\circ_{\mathrm{mic}}$, and isothermal compressibility, $\Delta\kappa^\circ_{\mathrm{mic}}$,[5,7,20,37]

$$\Delta G_{\mathrm{mic}} = \Delta G^\circ_{\mathrm{mic}} + \Delta V^\circ_{\mathrm{mic}}(P - P^\circ) - \frac{1}{2}\Delta\kappa^\circ_{\mathrm{mic}}(P - P^\circ)^2 \tag{6}$$

where $\Delta G^\circ_{\mathrm{mic}}$ is the standard free energy.

RESULTS AND DISCUSSION

Critical Micelle Concentration Determination from ^{1}H NMR Spectroscopy. From Figure 1, which shows the structures of the four detergents investigated here, it is evident that SDS, DPC, and DDM possess identical hydrophobic tails, indicated in red, while DPC and CyF possess identical head groups, shown in blue. The ^{1}H NMR spectra for all four detergents, at a concentration where the micellar state predominates, are provided in Supporting Information Figure S1, with corresponding assignments. All detergents were studied in 50 mM phosphate buffer, which is known to lower the cmc of anionic detergents. As may be ascertained from Supporting Information Table S1, ^{1}H chemical shifts are generally rather similar in the monomeric and micellar states, since these shifts primarily reflect chemical structure rather than topology. Nevertheless, certain resonances, highlighted in red in Supporting Information Table S1, exhibit significantly different chemical shifts in the monomeric versus micellar state, which renders them useful for evaluating the monomer−micelle equilibrium. In principle, any resonance for which the chemical shifts of the monomer and micelle phases are distinct could be used to determine the phase equilibrium. In practice, the ^{1}H chemical shift of C1 generally exhibits a robust upfield shift ($\Delta\delta_1$), while most aliphatic resonances (typically C12) shift downfield ($\Delta\delta_2$), upon formation of the micelle. For this reason, we characterized the monomer−micelle equilibrium by referencing the ^{1}H chemical shift of C1 to an aliphatic, such as C12, effectively measuring a difference of shifts, and thereby improving precision. Using eqs 1−3, and appropriate reference spectra above and below the cmc, the cmc is readily extracted from ^{1}H NMR spectra at a single detergent concentration in the vicinity of the cmc. Thus, from ^{1}H NMR spectra of 4.0 mM SDS, 2.0 mM DPC, 0.4 mM DDM, and 2.7 mM CyF, cmc values were obtained in this fashion for these four detergents with results as listed in Table 1.

The validity of this approach for determining detergent cmcs may be evaluated by comparing the results in Table 1 with established values. Specifically, the cmc of SDS measured here via ^{1}H NMR is in excellent agreement with values obtained under comparable conditions using fluorescence,[38] or calorimetry.[2,36] Likewise, the cmc of DPC, as determined via fluorescence measurements,[38,39] agrees well with the ^{1}H

Table 1. Thermodynamic[a] and Volumetric[b] Parameters for the Monomer−Micelle Equilibrium of the Detergents SDS, DPC, DDM, and CyF, Obtained from ^{1}H NMR Studies as a Function of Temperature and Pressure[c]

detergent	cmc[d] (mM)	$\Delta G^\circ_{\mathrm{mic}}$ (kJ mol^{-1})	$\Delta H^\circ_{\mathrm{mic}}$ (kJ mol^{-1})	$T\Delta S^\circ_{\mathrm{mic}}$ (kJ mol^{-1})	$\Delta C^\circ_{p,\mathrm{mic}}$ (kJ mol^{-1} K^{-1})	$\Delta V^\circ_{\mathrm{mic}}$ (mL mol^{-1})	$\Delta\kappa^\circ_{\mathrm{mic}}$ (mL mol^{-1} bar^{-1})[e]
SDS	1.60	−41	−1.4	39.8	−0.67	16.6	143
DPC	1.10	−27	9.4	36.2	−0.39	8.1	77
DDM	0.15	−32	3.8	35.6	−0.56	11.4	77
CyF	1.60	−26	9.4	35.0	−0.45	6.6	67

[a] $\Delta G^\circ_{\mathrm{mic}}$, $\Delta H^\circ_{\mathrm{mic}}$, $T\Delta S^\circ_{\mathrm{mic}}$, and $\Delta C^\circ_{p,\mathrm{mic}}$ were determined from the temperature dependence at constant pressure (1 bar), referenced to 298 K. [b] $\Delta V^\circ_{\mathrm{mic}}$ and $\Delta\kappa^\circ_{\mathrm{mic}}$ were determined from the pressure dependence at constant temperature (298 K), referenced to 1 bar. [c] Typical standard errors for the cmc, $\Delta G^\circ_{\mathrm{mic}}$, $\Delta H^\circ_{\mathrm{mic}}$, $T\Delta S^\circ_{\mathrm{mic}}$, $\Delta C^\circ_{p,\mathrm{mic}}$, $\Delta V^\circ_{\mathrm{mic}}$, and $\Delta\kappa^\circ_{\mathrm{mic}}$ are ±5, ±1, ±15, ±3, ±11, ±5, and ±7%. [d] At 298 K and 1 bar pressure. [e] ×10^{-4}

dx.doi.org/10.1021/jp500139p | J. Phys. Chem. B 2014, 118, 5698−5706

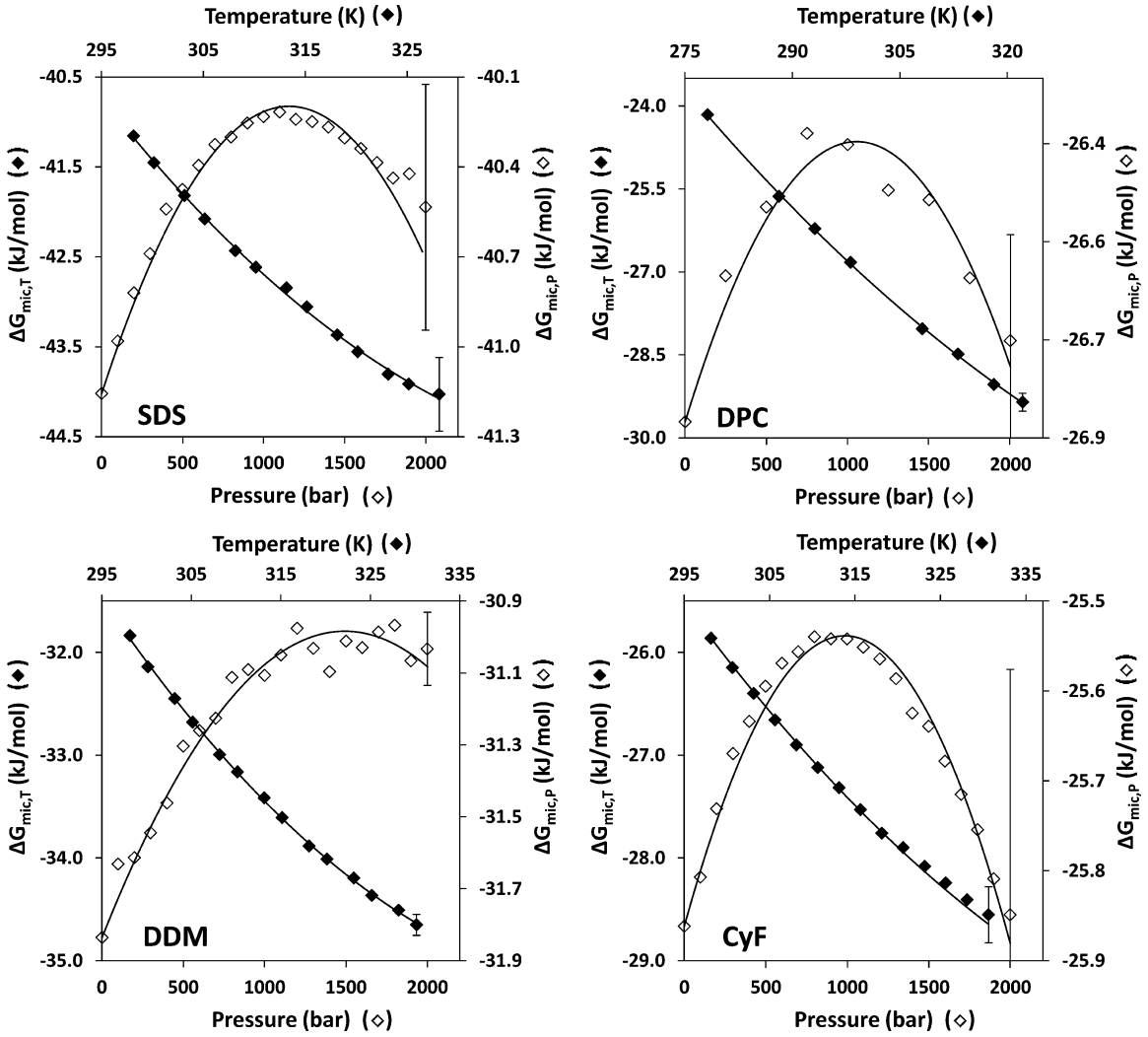

Figure 3. Temperature and pressure dependence of the Gibbs free energy of micellization for SDS, DPC, DDM, and CyF as obtained using NMR. The temperature dependence was measured at 1 bar, while the pressure dependence was measured at 298 K. Conservative estimates of the percent error in ΔG° values was typically 0.5−1% for all detergents. Sample error bars are provided for the last point of all data series.

NMR result obtained here. Further, the cmc of DDM as reported by De Grip and Bovee-Geurts[40] is in excellent agreement with our value. The one exception is the case of CyF, where the cmc we report in Table 1 is roughly 2.5 times that listed on the Anatrace Web site (no literature value was found). The Anatrace value was obtained in water, while we employed 50 mM phosphate buffer.

Temperature and Pressure Dependence of the Monomer−Micelle Equilibrium. Figure 3 shows the temperature and pressure dependence of the Gibbs free energy of micellization, ΔG°_{mic}, for all four detergents, on the basis of ^{1}H NMR chemical shift measurements of X_{mon} as previously described and with application of eq 4. The degree of counterion binding, f, for SDS was assumed to be 0.59.[36] It is useful to note that varying sodium concentrations, for SDS, are anticipated to impact X_{mon} rather than f.[41] In the figure, the solid lines represent fits of the temperature and pressure dependence of ΔG°_{mic} to eqs 5 and 6. The thermodynamic, ΔH°_{mic}, ΔS°_{mic}, and $\Delta C^\circ_{p,mic}$, and volumetric, ΔV°_{mic} and $\Delta \kappa^\circ_{mic}$, fitting parameters so obtained are listed in Table 1.

Where literature values are available, the thermodynamic parameters in Table 1 compare well. For SDS, for example, the values of ΔG°_{mic}, ΔH°_{mic}, and $T\Delta S^\circ_{mic}$ reported by Paula et al.[2] are found to equal −41.3, 3.0, and 38.3 kJ mol^{-1}, respectively, after adjusting for counterion binding (f = 0.59) and, thus, are in good agreement with Table 1. Similarly, heat capacity changes and volumetric parameters for SDS agreed well with reported values.[36,42] Likewise, specific volume changes for DDM were comparable to those reported for the structurally similar detergent decyl maltoside.[3] No other thermodynamic or volumetric parameters were found, particularly for CyF.

Comparing these four different detergents, the thermodynamic data demonstrate that, in all cases, micelle formation is entropically driven and the favorable entropy of micellization is roughly the same for each detergent. The positive entropy change reflects the significant release of waters of hydration to the bulk phase upon formation of the micelle, which outweighs the loss of configurational entropy of detergents confined to a the micelle in comparison to the bulk phase.[19,33,43]

While micelle formation is an entropically driven process, the enthalpy change associated with micelle formation is in fact positive for the three nonionic detergents investigated but slightly negative for SDS. Since interchain van der Waals contacts are expected to be favorable upon insertion of a detergent into a micelle, the overall positive enthalpy change must reflect changes in the hydration enthalpy upon release of

dx.doi.org/10.1021/jp500139p | J. Phys. Chem. B 2014, 118, 5698−5706

the hydration cage associated with the alkyl chains in the monomer phase.[19,33,43] In the case of SDS, the additional consideration of sodium ion binding at the micelle surface and associated release of waters of hydration complicates the interpretation.

Heat capacity changes are also clearly apparent from the temperature-dependent fits of free energy of micellization. Generally, heat capacity changes are dictated by the change in apolar surface area through burial of the chains in the micelle. Allowing for 57 J mol^{-1} K^{-1} per methylene group, we would expect to observe a negative heat capacity on the order of −700 J mol^{-1} K^{-1}, assuming all methylene groups on the alkyl chain are fully buried. While this number is indeed comparable to that observed for the detergents studied, as shown in Table 1, the slightly reduced values for the heat capacity changes, particularly for DPC, likely reflect the fact that some methylene groups are not fully buried in the micelle hydrophobic interior.[3] We consider below the possibility that such heat capacity changes should relate to the hydrophobicity of the various detergents in their micellar state. This can be examined by comparing spectroscopically determined hydrophobicity gradients with the measured heat capacity changes, as discussed below.

Detergent Topology. Although the sensitivity of the ^{1}H chemical shift of C1 to the equilibrium state clearly shows that it is possible to make use of such shifts to assess monomer−micelle equilibria, resolution of individual positions along the alkyl chains is rather limited. On the other hand, in a two-dimensional ^{13}C/^{1}H chemical shift correlation experiment, it becomes possible to resolve the majority of resonances and explore position-specific changes. For example, Figure 4 shows

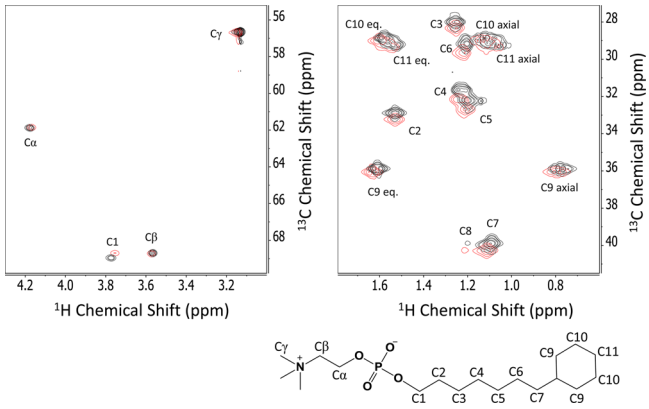

Figure 4. ^{1}H,^{13}C HMQC spectra of CyF showing methylene-specific changes in chemical shifts upon micellization of mainly headgroup (left) and alkyl tail (right) spectral regions. Peak assignments are as indicated on the spectra, which were collected from a sample in the micellar state (red; 30.8 mM) and a sample containing partial monomeric character, a 50:50 micelle:monomer sample (black; 3.47 mM). Using the frequency information from these two spectra, the pure monomeric chemical shifts were extracted using the weighted chemical shift equation (eq 2).

a comparison between ^{1}H,^{13}C HMQC spectra of CyF in the monomeric versus the micellar state, demonstrating that each of the alkyl chain and choline headgroup resonances are resolvable.

Figure 5 maps the chemical shift differences, $\Delta\delta$, between the monomer and micelle phases for each of the CyF carbons as obtained using the ^{13}C and ^{1}H chemical shifts measured from

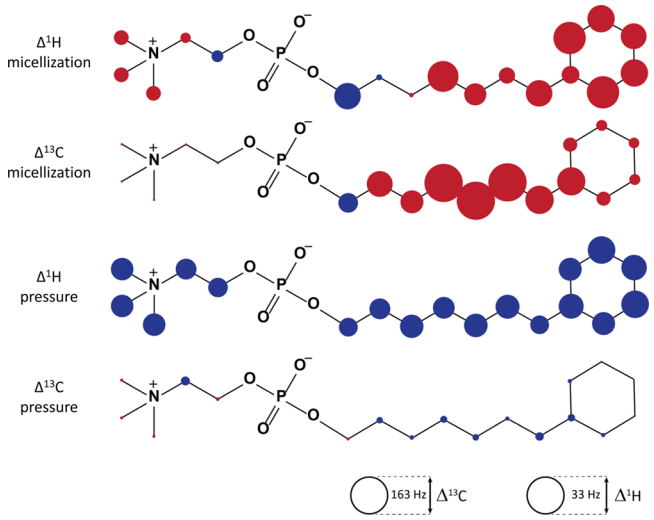

Figure 5. ^{1}H and ^{13}C chemical shift changes of CyF groups upon micellization and pressure perturbations obtained from ^{1}H, ^{13}C HMQC spectra at 25 °C. The magnitude of the chemical shift changes are represented by the diameter of the spheres, whose ^{1}H and ^{13}C scales are given. Positive shift changes are indicated in red and negative shift changes in blue, upon either micellization or pressure increase. Chemical shifts, associated with micellization, were obtained from mixed monomer/micelle and micelle samples, (3.47 and 30.8 mM, respectively). The chemical shift of the monomer was back-calculated using a weighted equation. Similarly, pressure maps were generated from the shift difference at 1 and 2000 bar, at a CyF concentration of 100 mM, where the micelle phase dominated.

the HMQC spectra in Figure 4. These chemical shift differences are represented by spheres with dimensions proportional to the magnitude of the particular ^{1}H and ^{13}C shifts and a color designating the sign of the chemical shift change. The aliphatic ^{1}H and ^{13}C shift differences are far more pronounced than those in the headgroup, with the exception of C1, whose anomalous shift change is in fact used to monitor the monomer−micelle equilibrium.

Environmental/solvent changes (aqueous to alkyl), structural ordering, and packing changes are among the complex contributions to the chemical shift changes observed upon micellization. It is likely that the dominant contributor in the alkyl tail is a change from an aqueous to an alkyl environment, characterized by positive changes in chemical shifts. Indeed, such positive changes in proton chemical shifts are observed for the C3−C12 alkyl regions of SDS, DPC, and DDM (Supporting Information Table S1).[9,28] The magnitude is likely modulated by structural ordering of the tail and packing effects. In addition to the chemical shift differences examined here, many other structural and dynamical properties can be measured by NMR, and these can provide insight into average conformations as well as both amplitudes and frequencies of conformational dynamics.

A further microscopic perspective on micellar topology may be obtained by examining the pressure response. The ^{13}C and ^{1}H chemical shift perturbations of CyF resulting from the application of a hydrostatic pressure of 2000 bar, at 25 °C, are also shown in Figure 5 (HMQC data are in Supporting Information Figure S2). In this case, shift perturbations arising from changes in the monomer−micelle equilibrium were effectively avoided by resorting to a high detergent concentration, where the equilibrium is strongly weighted toward the

dx.doi.org/10.1021/jp500139p | J. Phys. Chem. B 2014, 118, 5698−5706

micelle state. The largest shift perturbations are expected to arise from those moieties exhibiting the greatest conformational or topological changes. At higher pressures, these shifts are expected in regions with the greatest compressibility, which are likely to be those regions of lowest density (*i.e.*, the aliphatic groups of the acyl chains). Note that the pressure-induced changes in ^{1}H and, to a greater extent, ^{13}C chemical shifts exhibit an odd−even effect for the entirety of the methylene resonances associated with the acyl chains. Previous studies of lipids have identified odd−even effects in S_{CC} and S_{CH} orientational order parameters associated with acyl chains.[44] This was later attributed to packing effects and the alternation of gauche conformers along the chain.[45] Presumably, the introduction of pressure to the CyF micelle causes changes in acyl chain packing and the distribution of gauche conformers, reflected in ^{1}H and ^{13}C chemical shift changes. Thus, the spectra provide a hint as to the origin of compressibility changes, which we measure through the monomer−micelle equilibrium experiments (*vide infra*).

Since micelle formation is driven by the hydrophobic effect, it is instructive to examine the relative hydrophobicity throughout the micelle interior. We are most familiar with hydrophobicity from the perspective of measuring partitioning properties of a species of interest between two immiscible liquid phases—one hydrophobic and the other hydrophilic. In this application, we interpret hydrophobicity in terms of relative partitioning of a small paramagnetic probe, whose chemical potential dictates the extent to which it partitions between water and various depths in the micelle interior. Greater site-specific paramagnetic effects (shifts or relaxation rates) reflect local concentrations of paramagnetic probe and thus, hydrophobicity. Here, we rely upon the ^{1}H spectra to provide atomic resolution of the detergent micelle and a small hydrophobic paramagnetic probe, dioxygen, whose local partitioning can be measured through ^{1}H spin−lattice relaxation rates or ^{13}C contact shifts.[25,30,46] The extent to which oxygen partitions between the water bulk phase and the micelle interior will depend on the difference in chemical potential in each domain, which we relate primarily to hydrophobicity. Differences in O_2 collisional accessibility also affect the distribution of paramagnetic effects. To some extent, these effects can be accounted for by comparing the distribution of paramagnetic effects seen for the detergent below the cmc. At the very least, measuring paramagnetic effects from the partitioning of oxygen through the micelle provides a qualitative description of the hydrophobicity profile. Such profiles, obtained from ^{1}H NMR relaxation rate measurements in O_2, are provided in Table 2. At higher temperatures, the hydrophobicity associated with the micelle interior increases and the hydrophobicity gradients become more distinct between the different detergents. Additionally, the hydrophobicity appears to be greatest for those detergents with the lowest cmc. This trend likely reflects the fact that, in cases where the cmc is low, less detergent exchange (between the micelle and aqueous phase) takes place and, thus, less water is likely to penetrate the hydrophobic core of the micelle, resulting in a larger overall hydrophobicity gradient.

The above experiments involving chemical shift perturbations and paramagnetic effects from dissolved oxygen demonstrate how NMR spectroscopy can be used to provide a detailed perspective on structure, dynamics, and topology. Ultimately, these microscopic effects must be reflected in the thermodynamic and volumetric properties of the system, which we discuss below.

Table 2. Estimates of Hydrophobicity Quotients, Defined by the Ratio of the ^{1}H Paramagnetic Relaxation Rate of a Site of Interest on the Detergent to That of H_2O, at a Fixed Oxygen Partial Pressure[a]

	hydrophobicity quotient							
	25 °C				50 °C			
carbon group	SDS	DPC	DDM	CyF	SDS	DPC	DDM	CyF
Cγ		1.4		1.6		1.8		1.9
Cβ		1.4		1.6		1.9		2.0
Cα		1.6		1.8		2.3		2.5
C1	2.6	2.7		2.7	3.3	3.8		3.9
C2	3.0	3.1	3.7	3.3	3.7	4.4	4.8	4.5
C3−C11	3.4	3.5	4.4		4.4	5.3	6.6	
C12	4.0	4.2	5.0		5.0	6.0	7.3	

[a]Oxygen will partition preferentially into more hydrophobic environments, giving rise to enhanced relaxation and a higher hydrophobicity quotient.

Connecting Thermodynamic Properties with Microscopic Features of the System. While the distribution of O_2 in the micelle is determined by hydrophobicity, excluded volume or collisional accessibility will also influence the observed distribution. In principle, the two parameters can be distinguished by employing a separate probe of similar size, such as water.[31] The relative partitioning of water across the micelle can be spectroscopically identified through solvent isotope shifts or water NOESY contacts to the nuclei of interest.[25,30,47] Since water and oxygen are comparable in size, their differences in partitioning result largely from differences in chemical potential. For the current study, we confine our analysis to ^{1}H paramagnetic relaxation rates, arising from O_2, and attribute the bulk of the differences in partitioning to gradations in hydrophobicity. We further define an experimental hydrophobicity quotient as the paramagnetic rate, associated with the presence of oxygen, acting on a species of interest divided by the corresponding rate on water itself. Since the change in heat capacity and our quotient are both manifestations of the hydrophobicity of the micelle environment, there should exist a relationship between these two hydrophobic rulers. Indeed, Figure 6 shows such a strong correlation (R^2 = 0.9995) between our experimentally determined average chain hydrophobicity and the measured heat capacity change, for the nonionic detergents. Presumably, chains which exhibit greater heat capacities associated with micellization, do so because desolvation energies are larger; this would be expected for chains exhibiting greater hydrophobicity.

The pressure dependence of the free energy of micellization reveals a clear positive change in the partial molar volume associated with formation of the micelle. The release of waters of hydration again contributes to partial molar volume changes. SDS, in particular, exhibits a pronounced increase in the partial molar volume associated with formation of the micelle. Waters associated with sodium ions are liberated, as the micelle state is adopted and sodium ions preferentially interact with the micelle surface, thereby serving to screen electrostatic repulsion between SDS headgroups. Compressibility changes are positive and are observed to be very similar, with the exception of SDS whose molar compressibility difference is largest. It has been previously noted that the compressibilities of the hydrocarbon interior of most detergents are similar to those observed in pure

dx.doi.org/10.1021/jp500139p | J. Phys. Chem. B 2014, 118, 5698−5706

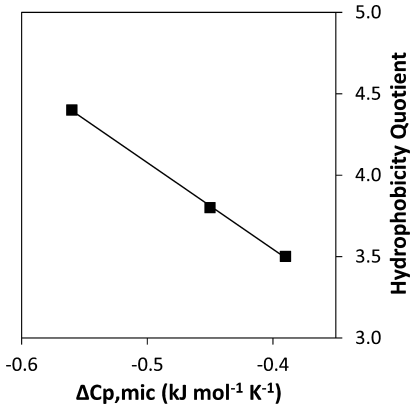

Figure 6. Heat capacity change, $\Delta C_{p,\mathrm{mic}}$, as a function of average hydrophobicity for nonionic detergents. The site-specific hydrophobicity is simply defined by the partition coefficient of oxygen between water and the site of interest in the micelle. The partition coefficients are in turn determined by paramagnetic rate measurements on both water and the nucleus of interest. An average chain hydrophobicity was then determined by averaging these experimentally determined quotients for all protons constituting the detergent chain.

hydrocarbon phases. Thus, the increased compressibility difference observed with SDS may arise from a significant compressibility effect associated with the headgroup region, which undergoes a pronounced conformational change, upon formation of the micelle.

In summary, NMR spectroscopy represents a sensitive and rapid method to discern detergent micelle phase equilibria, while details of chemical shift changes, relaxation rates, and the effects of paramagnetic additives provide a topological description. Together, a statistical mechanical perspective of the thermodynamic and volumetric parameters associated with the formation of the micelle phase can be obtained. There are many nuances associated with detergent behavior that are of great interest to the scientific community. For example, the use of specific detergents or detergent mixtures to stabilize membrane proteins remains somewhat of a black art. Detergents also exhibit exotic phases as mixtures or under different conditions of solvent, salt, and concentration. In principle, the systematic approach of phase equilibria and detailed spectroscopic studies should provide insight into the physical chemistry of many aspects of detergent behavior.

MATERIALS AND METHODS

Sodium *n*-dodecyl sulfate (SDS) was obtained from BioShop Canada Inc. (Burlington, Ontario, Canada), and *n*-dodecyl phosphocholine (DPC) was obtained from Avanti Polar Lipids Inc. (Alabaster, AL, USA). *n*-Dodecyl-β-D-maltoside (DDM) and cycloFos-7 (CyF) were obtained from Affymetrix (Santa Clara, CA, USA). All chemicals were used without further purification. NMR samples, used to acquire thermodynamic and volumetric data, were prepared by mixing the respective detergents with phosphate buffer (50 mM, pH 8, 99.9% D_2O). For each detergent, samples were prepared at concentrations corresponding to monomeric (well below the cmc), mixed micelle/monomer (2 × cmc), and micelle (well above the cmc) states, respectively, as follows: SDS was prepared at 0.2, 4, and 40 mM, DPC at 0.2, 2, and 10 mM, DDM at 0.04, 0.4, and 4 mM, and CyF at 0.12, 2.7, and 30 mM. CyF samples used to obtain chemical shift maps of micellization were 3.47 and 30.8 mM, reflecting monomer and micelle states, respectively; 100 mM CyF was used to assess pressure perturbations.

NMR experiments were performed on a 600 MHz Varian Inova spectrometer (Agilent Technologies, Santa Clara, CA, USA) using a cryogenic HCN probe, capable of being separately tuned to FCN. In the case of oxygen paramagnetic rate measurements, the sample was pressurized in a 5 mm o.d. sapphire NMR tube (Saphikon, NH) to 20 bar oxygen partial pressure. Typically, ^{1}H NMR experiments were acquired at each temperature and pressure point, with 16−64 transients, while measurements below the cmc required as many as 256 transients. Generally, the acquisition time was 2 s, the spectral width 12 kHz, and the raw free induction decay (FID) size was 48 kB. Spectra were processed with standard 1 Hz Lorentzian apodization. Typical ^{13}C and ^{1}H 90° pulse lengths were 16 and 8 μs, respectively, while most ^{13}C,^{1}H HMQC spectra were obtained using 48−384 scans, 256 increments, a spectral width of 10 kHz in the indirect dimension, and a repetition time of 1.2 s. A gradient version of the HMQC was used to observe ^{1}H and ^{13}C chemical shift changes at pressures of 1 and 2000 bar at 25 °C. Spectral analysis and peak deconvolution were performed using Mestrenova (Mestrelab Research, Santiago de Compostela, Spain).

DATA ANALYSIS

The cmc mole fraction, X_{mon}, was determined from ^{1}H NMR spectra, using eq 3. For each temperature and pressure point, three detergent concentrations were examined corresponding to approximately 10× below the cmc, 2× above the cmc, and 20× above the cmc, as previously detailed. This permitted the simultaneous determination of δ_{mon}, δ_{obs}, δ_{mic}, and, therefore, X_{mon}, at each temperature and pressure point. Phase equilibria can in principle be determined from any resonance in the spectra. However, to maximize the precision and sensitivity of the cmc determination, the difference between the chemical shift of C1 and a second resolved resonance was typically measured. Since each of the two resonances exhibits opposite chemical shift trends as a function of X_{mon}, the difference between the shifts avoids the need for a chemical shift standard (which may exhibit a weak interaction with the micelle or detergents) while providing a more robust measure of the equilibrium through amplification of the difference in chemical shift between observed phases. For example, for SDS and DPC at any one temperature and pressure, the mole fraction of monomer was calculated using information from both the C1 and C12 peaks in the alkyl tail,

$$X_{\mathrm{mon}} = \frac{(\delta_{\mathrm{C1}} - \delta_{\mathrm{C12}})_{\mathrm{obs}} - (\delta_{\mathrm{C1}} - \delta_{\mathrm{C12}})_{\mathrm{mic}}}{(\delta_{\mathrm{C1}} - \delta_{\mathrm{C12}})_{\mathrm{mic}} - (\delta_{\mathrm{C1}} - \delta_{\mathrm{C12}})_{\mathrm{mon}}} \quad (7)$$

A similar procedure was employed for DDM and CyF, where the specific resonances used in the analysis are noted in Supporting Information Table S1 (highlighted in red). Typically, the full widths at half-maxima (fwhm) for the C1 and C12 resonances of SDS were 4.5 and 5 Hz, respectively, while those for DPC were 4 and 3.5 Hz, respectively. For DDM the fwhm were 9.5 and 6 Hz for the C1′ and an unassigned headgroup resonance (~3.277 ppm), respectively, and were 6 and 4 Hz for the CyF C1 and Cy peaks. In every case, both resonances were completely resolved and could therefore be defined to within a small fraction of the line width. Using the method of difference of shifts, the overall changes in chemical shift differences between monomeric and micellar states were

dx.doi.org/10.1021/jp500139p | J. Phys. Chem. B 2014, 118, 5698−5706

37, 39, 77, and 40 Hz, respectively, for SDS, DPC, DDM, and CyF.

In creating the chemical shift maps upon micellization for CyF (Figure 5), a roughly 50:50 monomer:micelle CyF sample was chosen to reflect the monomeric state, as the HMQC signal observed from the pure monomer sample was low. Assuming a two-phase model for micelle formation and given fast detergent exchange between phases, the observed chemical shifts in this sample will be a weighted average of the true monomer and micelle chemical shifts (eq 2) and thus contain 50% monomeric character. Consequently, the chemical shift changes upon micellization will be twice as great as that observed in Figure 4, and the monomer chemical shift can be obtained using eq 3. Additionally, in the ^{1}H chemical shift maps, the displayed value in the cyclohexyl region is an average of the axial and equatorial chemical shift changes.

Upon determining X_{mon} as previously described, the free energy could then be calculated using eq 3. The thermodynamic and volumetric parameters could then be ascertained by fitting the experimentally determined temperature- and pressure-dependent free energy profiles to eqs 5 and 6, respectively. In some cases, it proved more reliable to determine the thermodynamic parameters from an analysis of the temperature dependence of ln X_{cmc} and f,[2,36] where

$$\ln X_{cmc} = aT^2 + bT + c \tag{8}$$

$$f = a'T^2 + b'T + c' \tag{9}$$

The enthalpy term, ΔH°_{mic}, is described via

$$\Delta H^\circ_{mic} = -RT^2\left[(1+f)\left(\frac{\mathrm{d}\ln X_{cmc}}{\mathrm{d}T}\right) + \ln X_{cmc}\,\frac{\mathrm{d}f}{\mathrm{d}T}\right] \tag{10}$$

If it is assumed that $(\mathrm{d}f/\mathrm{d}T)$ is not significant, as appears the case for SDS,[48,49] this expression reduces to eq 11.

$$\Delta H^\circ_{mic} = -RT^2[(1+f)(2aT+b)] \tag{11}$$

The entropy change is then simply

$$\Delta S^\circ_{mic} = \frac{\Delta G^\circ_{mic} - \Delta H^\circ_{mic}}{T} \tag{12}$$

while the heat capacity change associated with the monomer to micelle transition is

$$\Delta C^\circ_{p,mic} = \frac{\mathrm{d}\Delta H^\circ_{mic}}{\mathrm{d}T} = -R(1+f)(6aT^2 + 2bT) \tag{13}$$

■ ASSOCIATED CONTENT

Supporting Information

Figures showing ^{1}H NMR spectra of SDS, DPC, DDM and CyF with assignments and ^{1}H,^{13}C HMQC spectra of CyF before and after a pressure perturbation and a table listing chemical shifts of the monomeric and micellar states. This material is available free of charge via the Internet at http://pubs.acs.org.

■ AUTHOR INFORMATION

Corresponding Author

*E-mail: scott.prosser@utoronto.ca. Tel.: 905 828 3802. Fax: 905 828 5425.

Present Address

[‖]Laboratory Medicine and Pathobiology, Sunnybrook Hospital, Toronto, Ontario, Canada M4N 3M5.

Notes

The authors declare no competing financial interest.

■ ACKNOWLEDGMENTS

We would like to thank Prof. Heiko Heerklotz for his thoughtful comments and Harkeerat Bhatia for assisting with DPC controls. R.S.P. and P.M.M. acknowledge NSERC (Canada) for Discovery Awards.

■ ABBREVIATIONS

CyF 7-cyclohexyl-1-heptylphosphocholine
DDM *n*-dodecyl-*β*-D-maltoside
DPC *n*-dodecylphosphocholine
SDS sodium *n*-dodecyl sulfate
NMR nuclear magnetic resonance

■ REFERENCES

(1) Majhi, P. R.; Blume, A. Thermodynamic Characterization of Temperature-Induced Micellization and Demicellization of Detergents Studied by Differential Scanning Calorimetry. *Langmuir* **2001**, *17* (13), 3844−3851.

(2) Paula, S.; Sus, W.; Tuchtenhagen, J.; Blume, A. Thermodynamics of Micelle Formation as a Function of Temperature—A High-Sensitivity Titration Calorimetry Study. *J. Phys. Chem.* **1995**, *99* (30), 11742−11751.

(3) Fan, H. Y.; Nazari, M.; Chowdhury, S.; Heerklotz, H. Volume and Expansivity Changes of Micelle Formation Measured by Pressure Perturbation Calorimetry. *Langmuir* **2011**, *27* (5), 1693−1699.

(4) Perez-Rodriguez, M.; Prieto, G.; Rega, C.; Varela, L. M.; Sarmiento, F.; Mosquera, V. A Comparative Study of the Determination of the Critical Micelle Concentration by Conductivity and Dielectric Constant Measurements. *Langmuir* **1998**, *14* (16), 4422−4426.

(5) Moghaddam, M.; Chan, H. Pressure and Temperature Dependence of Hydrophobic Hydration: Volumetric, Compressibility, and Thermodynamic Signatures. *J. Chem. Phys.* **2007**, *126*, 114507.

(6) Vikingstad, E.; Skauge, A.; Hoiland, H. Effect of Pressure and Temperature on the Partial Molal Volume and Compressibility of Sodium Decanoate Micelles. *J. Colloid Interface Sci.* **1979**, *72* (1), 59−67.

(7) Lesemann, M.; Thirumoorthy, K.; Kim, Y. J.; Jonas, J.; Paulaitis, M. E. Pressure Dependence of the Critical Micelle Concentration of a Nonionic Surfactant in Water Studied by ^{1}H-NMR. *Langmuir* **1998**, *14* (19), 5339−5341.

(8) Sarac, B.; Cerkovnik, J.; Ancian, B.; Meriguet, G.; Roger, G. M.; Durand-Vidal, S.; Bester-Rogac, M. Thermodynamic and NMR Study of Aggregation of Dodecyltrimethylammonium Chloride in Aqueous Sodium Salicylate Solution. *Colloid Polym. Sci.* **2011**, *289* (14), 1597−1607.

(9) Landry, J. M.; Marangoni, D. G.; Lumsden, M. D.; Berno, R. 1D and 2D NMR Investigations of the Micelle-Formation Process in 8-Phenyloctanoate Micelles. *Can. J. Chem.* **2007**, *85* (3), 202−207.

(10) Wang, T. Z.; Mao, S. Z.; Miao, X. J.; Zhao, S.; Yu, J. Y.; Du, Y. R. H-1 NMR Study of Mixed Micellization of Sodium Dodecyl Sulfate and Triton X-100. *J. Colloid Interface Sci.* **2001**, *241* (2), 465−468.

(11) Furo, I. NMR Spectroscopy of Micelles and Related Systems. *J. Mol. Liq.* **2005**, *117* (1−3), 117−137.

(12) Soderman, O.; Stilbs, P.; Price, W. S. NMR Studies of Surfactants. *Concepts Magn. Reson., Part A* **2004**, *23A* (2), 121−135.

(13) Bolt, J. D.; Turro, N. J. Measurement of the Rates of Detergent Exchange between Micelles and the Aqueous Phase Using Phosphorescent Labeled Detergents. *J. Phys. Chem.* **1981**, *85* (26), 4029−4033.

(14) Phillips, J. N. The Energetics of Micelle Formation. *Trans. Faraday Soc.* **1955**, *51* (4), 561−569.
(15) Tanford, C. Micelle Shape and Size. *J. Phys. Chem.* **1972**, *76* (21), 3020−3024.
(16) Aniansson, E. A. G.; Wall, S. N. Kinetics of Step-Wise Micelle Association. *J. Phys. Chem.* **1974**, *78* (10), 1024−1030.
(17) Kresheck, G. C.; Hargrave, Wa Thermometric Titration Studies of Effect of Head Group, Chain-Length, Solvent, and Temperature on Thermodynamics of Micelle Formation. *J. Colloid Interface Sci.* **1974**, *48* (3), 481−493.
(18) Tanford, C. Theory of Micelle Formation in Aqueous Solutions. *J. Phys. Chem.* **1974**, *78* (24), 2469−2479.
(19) Lindman, B.; Wennerstrom, H.; Gustavsson, H.; Kamenka, N.; Brun, B. Some Aspects on the Hydration of Surfactant Micelles. *Pure Appl. Chem.* **1980**, *52* (5), 1307−1315.
(20) Offen, H. W. Micelles Under Pressure. *Rev. Phys. Chem. Jpn.* **1980**, *50* (1), 97−118.
(21) Mazer, N. A.; Olofsson, G. Calorimetric Studies of Micelle Formation and Micellar Growth in Sodium Dodecyl Sulfate Solutions. *J. Phys. Chem.* **1982**, *86* (23), 4584−4593.
(22) Cavanagh, J.; Fairbrother, W. J.; Palmer, A. G. I.; Skelton, N. J. *Protein NMR Spectroscopy: Principles and Practice*, 2nd ed.; Elsevier/Academic Press: Amsterdam, Boston, 2007.
(23) Marsh, J. A.; Singh, V. K.; Jia, Z. C.; Forman-Kay, J. D. Sensitivity of Secondary Structure Propensities to Sequence Differences Between Alpha- and Gamma-Synuclein: Implications for Fibrillation. *Protein Sci.* **2006**, *15* (12), 2795−2804.
(24) Niccolai, N.; Spiga, O.; Bernini, A.; Scarselli, M.; Ciutti, A.; Fiaschi, I.; Chiellini, S.; Molinari, H.; Temussi, P. A. NMR Studies of Protein Hydration and TEMPOL Accessibility. *J. Mol. Biol.* **2003**, *332* (2), 437−447.
(25) Al-Abdul-Wahid, M. S.; Evanics, F.; Prosser, R. S. Dioxygen Transmembrane Distributions and Partitioning Thermodynamics in Lipid Bilayers and Micelles. *Biochemistry* **2011**, *50* (19), 3975−3983.
(26) Al-Abdul-Wahid, M. S.; Verardi, R.; Veglia, G.; Prosser, R. S. Topology and Immersion Depth of an Integral Membrane Protein by Paramagnetic Rates from Dissolved Oxygen. *J. Biomol. NMR* **2011**, *51* (1−2), 173−183.
(27) Brown, W.; Pu, Z.; Rymden, R. Size and Shape of Nonionic Amphiphile Micelles: NMR Self-Diffusion and Static and Quasi-Elastic Light-Scattering Measurements on C12E5, C12E7, and C12E8 in Aqueous Solution. *J. Phys. Chem.* **1988**, *92* (21), 6086−6094.
(28) Svard, M.; Schurtenberger, P.; Fontell, K.; Jonsson, B.; Lindman, B. Micelles, Vesicles, and Liquid Crystals in the Monoolein-Sodium Taurocholate-Water System: Phase-Behavior, NMR, Self-Diffusion, and Quasi-Elastic Light Scattering Studies. *J. Phys. Chem.* **1988**, *92* (8), 2261−2270.
(29) Manzo, G.; Carboni, M.; Rinaldi, A. C.; Casu, M.; Scorciapino, M. A. Characterization of Sodium Dodecylsulphate and Dodecylphosphocholine Mixed Micelles through NMR and Dynamic Light Scattering. *Magn. Reson. Chem.* **2013**, *51* (3), 176−183.
(30) Al-Abdul-Wahid, M.; Yu, C.; Batruch, I.; Evanics, F.; Pomes, R.; Prosser, R. A Combined NMR and Molecular Dynamics Study of the Transmembrane Solubility and Diffusion Rate Profile of Dioxygen in Lipid Bilayers. *Biochemistry* **2006**, *45* (35), 10719−10728.
(31) Evanics, F.; Hwang, P. M.; Cheng, Y.; Kay, L. E.; Prosser, R. S. Topology of an Outer-Membrane Enzyme: Measuring Oxygen and Water Contacts in Solution NMR Studies of PagP. *J. Am. Chem. Soc.* **2006**, *128* (25), 8256−8264.
(32) Blandamer, M.; Cullis, P.; Soldi, L.; Engberts, J.; Kacperska, A.; Van Os, N.; Subha, M. Thermodynamics of Micellar Systems: Comparison of Mass Action and Phase Equilibrium Models for the Calculation of Standard Gibbs Energies of Micelle Formation. *Adv. Colloid Interface Sci.* **1995**, *58* (2−3), 171−209.
(33) Chachaty, C. Applications of NMR methods to the Physical-Chemistry of Micellar Solutions. *Prog. Nucl. Magn. Reson. Spectrosc.* **1987**, *19*, 183−222.
(34) Guo, W.; Fung, B.; O'Rear, E. Exchange of Hybrid Surfactant Molecules between Monomers and Micelles. *J. Phys. Chem.* **1992**, *96* (24), 10068−10074.
(35) Hadgiivanova, R.; Diamant, H. Premicellar Aggregation of Amphiphilic Molecules. *J. Phys. Chem. B* **2007**, *111* (30), 8854−8859.
(36) Chatterjee, A.; Moulik, S. P.; Sanyal, S. K.; Mishra, B. K.; Puri, P. M. Thermodynamics of Micelle Formation of Ionic Surfactants: A Critical Assessment for Sodium Dodecyl Sulfate, Cetyl Pyridinium Chloride and Dioctyl Sulfosuccinate (Na Salt) by Microcalorimetric, Conductometric, and Tensiometric Measurements. *J. Phys. Chem. B* **2001**, *105* (51), 12823−12831.
(37) Bezsonova, I.; Korzhnev, D. M.; Prosser, R. S.; Forman-Kay, J. D.; Kay, L. E. Hydration and Packing along the Folding Pathway of SH3 Domains by Pressure-Dependent NMR. *Biochemistry* **2006**, *45* (15), 4711−4719.
(38) Alvares, R. D. A.; Tulumello, D. V.; Macdonald, P. M.; Deber, C. M.; Prosser, R. S. Effects of a Polar Amino Acid Substitution on Helix Formation and Aggregate Size Along the Detergent-Induced Peptide Folding Pathway. *Biochim. Biophys. Acta, Biomembr.* **2013**, *1828* (2), 373−381.
(39) Macdonald, P. M.; Rydall, J. R.; Kuebler, S. C.; Winnik, F. M. Synthesis and Characterization of a Homologous Series of Zwitterionic Surfactants Based on Phosphocholine. *Langmuir* **1991**, *7* (11), 2602−2606.
(40) De Grip, W. J.; Bovee-Geurts, P. H. M. Synthesis and Properties of Alkylglucosides with Mild Detergent Action: Improved Synthesis and Purification of β-1-Octyl-, β-1-Nonyl-, and β-1-Decyl-glucose. Synthesis of β-1-Undecylglucose and β-1-Dodecylmaltose. *Chem. Phys. Lipids* **1979**, *23* (4), 321−335.
(41) Corrin, M. L.; Harkins, W. D. The Effect of Salts on the Critical Concentration for the Formation of Micelles in Colloidal Electrolytes. *J. Am. Chem. Soc.* **1947**, *69* (3), 683−688.
(42) Brun, T. S.; Hoiland, H.; Vikingstad, E. Partial Molal Volumes and Isentropic Partial Molal Compressibilities of Surface-Active Agents in Aqueous-Solution. *J. Colloid Interface Sci.* **1978**, *63* (1), 89−96.
(43) Chevalier, Y.; Zemb, T. The Structure of Micelles and Microelulsions. *Rep. Prog. Phys.* **1990**, *53* (3), 279−371.
(44) Douliez, J. P.; Leonard, A.; Dufourc, E. J. Conformational Order of DMPC sn-1 Versus sn-2 Chains and Membrane Thickness: An Approach to Molecular Protrusion by Solid State ^{2}H-NMR and Neutron Diffraction. *J. Phys. Chem.* **1996**, *100* (47), 18450−18457.
(45) Smondyrev, A. M.; Berkowitz, M. L. Molecular Dynamics Study of *sn*-1 and *sn*-2 Chain Conformations in Dipalmitoylphosphatidylcholine Membranes. *J. Chem. Phys.* **1999**, *110* (8), 3981−3985.
(46) Prosser, R. S.; Luchette, P. A.; Westerman, P. W. Using O-2 to Probe Membrane Immersion Depth by F-19 NMR. *Proc. Natl. Acad. Sci. U. S. A.* **2000**, *97* (18), 9967−9971.
(47) Al-Abdul-Wahid, M.; Neale, C.; Pomès, R.; Prosser, R. A Solution NMR Approach to the Measurement of Amphiphile Immersion Depth and Orientation in Membrane Model Systems. *J. Am. Chem. Soc.* **2009**, *131* (18), 6452−6459.
(48) Benrraou, M.; Bales, B. L.; Zana, R. Effect of the Nature of the Counterion on the Properties of Anionic Surfactants. 1. CMC, Ionization Degree at the CMC and Aggregation Number of Micelles of Sodium, Cesium, Tetramethylammonium, Tetraethylammonium, Tetrapropylammonium, and Tetrabutylammonium Dodecyl Sulfates. *J. Phys. Chem. B* **2003**, *107* (48), 13432−13440.
(49) Shah, S. S.; Jamroz, N. U.; Sharif, Q. M. Micellization Parameters and Electrostatic Interactions in Micellar Solution of Sodium Dodecyl Sulfate (SDS) at Different Temperatures. *Colloids Surf., A* **2001**, *178* (1−3), 199−206.